

DD

E1-97-324

A.K.Kacharava, V.I.Komarov, A.V.Kulikov,  
M.S.Nioradze<sup>1</sup>, G.G.Macharashvili, H.Müller<sup>2</sup>,  
A.Yu.Petrus, H.Seyfarth<sup>3</sup>, S.V.Yaschenko

EXPECTED CONDITIONS OF THE ANKE  
FORWARD DETECTOR OPERATION

SCAN-9801122



CERN LIBRARIES, GENEVA

<sup>1</sup>HEPI TSU, Tbilisi, Rep. of Georgia

<sup>2</sup>IKPH, FZ-Rossendorf, Dresden, Germany

<sup>3</sup>IKP, FZ-Jülich, Germany

sw 9805

## Introduction .

The Forward detector (FD) of the ANKE spectrometer was originally proposed for exclusive investigation of the deuteron break-up reaction  $pd \rightarrow ppn$  under the kinematic conditions far from the kinematics of quasi-free nucleon-nucleon interaction (cumulative break-up) ([1], [2]). In this experiment the momentum of fast protons, emitted at small angles with respect to the beam, is measured with a relatively low flux of the particles through the detectors, determined by a small thickness of the jet (or cluster) deuterium target. However, the requirements to the detector (acceptance, resolving power, counting rate capability, particle identification possibility) were not restricted by the demands of this experiment alone. Emission of secondary particles with high momenta at small angles is typical for many intermediate-energy processes. Therefore, the capability of their effective detection by the FD obviously improves the performance of the spectrometer as a whole.

Indeed, it was shown ([3]–[7]) that study of several specific processes demands a use of the Forward detector. Thus, the detector is definitely necessary for studying the following processes:

- (i) the cumulative deuteron break-up reaction ([1], [2])

$$p + d \rightarrow p + p + n \text{ at } T_p = 1000\text{--}2500 \text{ MeV}; \quad (1)$$

- (ii) subthreshold production of  $K^+$ -mesons and  $K^+K^-$  pairs [3]–[5], correlated with emission of light fragments in the forward cone of angles:

$$p + {}^{12}\text{C} \rightarrow (p, d) + K^+ + X \text{ at } T_p = 800\text{--}1500 \text{ MeV}; \quad (2)$$

$$p + {}^{12}\text{C} \rightarrow (p, d, {}^3\text{H}, {}^3\text{He}) + K^+ + K^- + X \text{ at } T_p = 2000\text{--}2500 \text{ MeV}; \quad (3),$$

- (iii) production of  $a_0^+$ -mesons [6] in the reaction:

$$p + p \rightarrow d + a_0^+ \rightarrow d + K^+ + \bar{K}^0 \text{ at } T_p = 2520 \text{ and } 2600 \text{ MeV}; \quad (4),$$

- (iv) search for the  $NN^*$ -component in the deuteron [7]:

$$p + d \rightarrow d + N^* \rightarrow d + n + \pi^+ \text{ at } T_p = 1500\text{--}2000 \text{ MeV}. \quad (5)$$

All the reactions (1)–(5) do not cover all permitted processes that are accompanied by emission of high-momentum particles at small angles and are currently of great interest in terms of physics. Nevertheless, they rather completely characterize the requirements to the ANKE Forward detector.

The purpose of the present paper is to study the capability of the FD to detect and identify the particles from reactions (1)–(5), proposed for investigation at the ANKE spectrometer.

The Monte Carlo simulation was used to study several of the main characteristics of the detector performance:

- (a) angular-momentum acceptance;
- (b) the counting rates for the processes of interest;
- (c) the accompanying background processes;
- (d) the possibility of using Cherenkov counters of total internal reflection (CTIR) [8];
- (e) the total background suppression factor, ensured by using of  $\Delta E$  and Cherenkov counters at the trigger level and time-of-flight (TOF) measurements during the off-line data processing.

### **Forward Detector Overview.**

The scheme of the ANKE setup is presented in **Fig. 1**. It consists of four detection systems: Forward detector (FD), Positive and Negative Side detectors (PSD and NSD), Backward detector (BD). The basic geometrical parameters of the detector systems are given in [5]. The FD [9] will be used in coincidence with the BD in the deuteron breakup study ([1], [2]), with the Side detector in the experiments on  $K^+$  and  $K^+K^-$  subthreshold production [3]–[5], and can also be used in other experiments [6],[7] that involve emission of fast particles in the forward direction. The Forward detector records fast positive particles emitted at small angles and leaving the dipole D2 through its forward boundary. The FD consists of 3 packages of narrow-gap proportional chambers (MWPC) [10] and two-plane scintillation hodoscope (FH) placed behind the MWPC. The first plane of this hodoscope consists of 8 elements, the second one of 9 elements. The elements have scintillators 20 and 15 mm thick, most of them are 80 mm wide. Several scintillators close to the beam pipe (2 in the first and 3 in the second plane) are less wide (40, 50, 60 mm) as the counting rate increases by a factor of about 3 at this side of the hodoscope.

The Forward detector has to record the track of a particle, to measure the ionization losses in both planes of the scintillation hodoscope and the time correlation with a particle detected in the Side or Backward detector.

It is also possible to use Cherenkov counters (CTIR) [8] for additional suppression of the background in the kinematic region where the  $\Delta E$  and TOF methods alone are not sufficient to identify particles. The Cherenkov counters are installed behind the scintillation hodoscope (unlike the case in the detector scheme considered in [9], where aerogel Cherenkov counters were supposed to be used).

### **Types of the Particles Detected in FD.**

Table 1 lists the types of secondary particles to be detected in the FD in the planned measurements([2]–[7]) depending on the energy of the initial particle.

The angular-momentum (geometrical) acceptance of the FD for two typical values of incident energy and D2 magnetic field is shown in **Fig. 2**. The geometrical acceptance has been obtained at homogeneously generated ejectiles in the phase space corresponding to  $P_{eject} = 0 \div 4000 \text{ MeV}/c$  and emission angles  $\vartheta \leq 10^\circ$ .

Particles were considered as detected if they reached the second plane of the scintillation hodoscope. All secondary processes, like decay in flight, multiple Coulomb scattering and hadronic interactions, were switched off in the simulation.

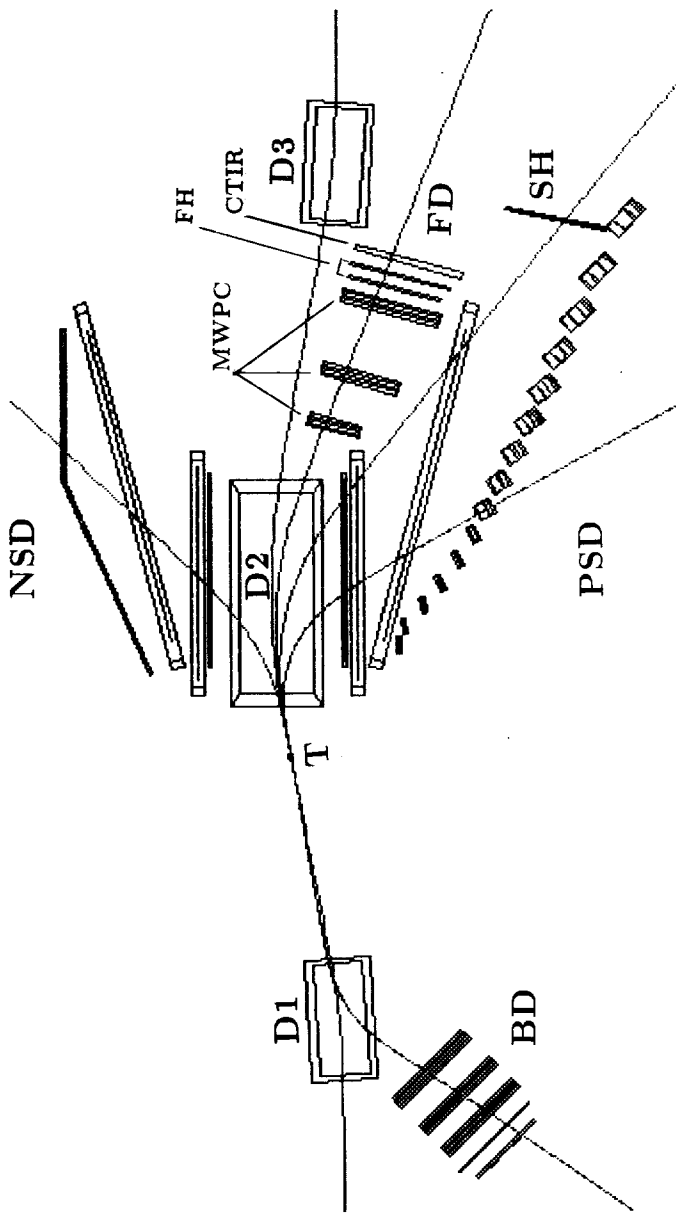
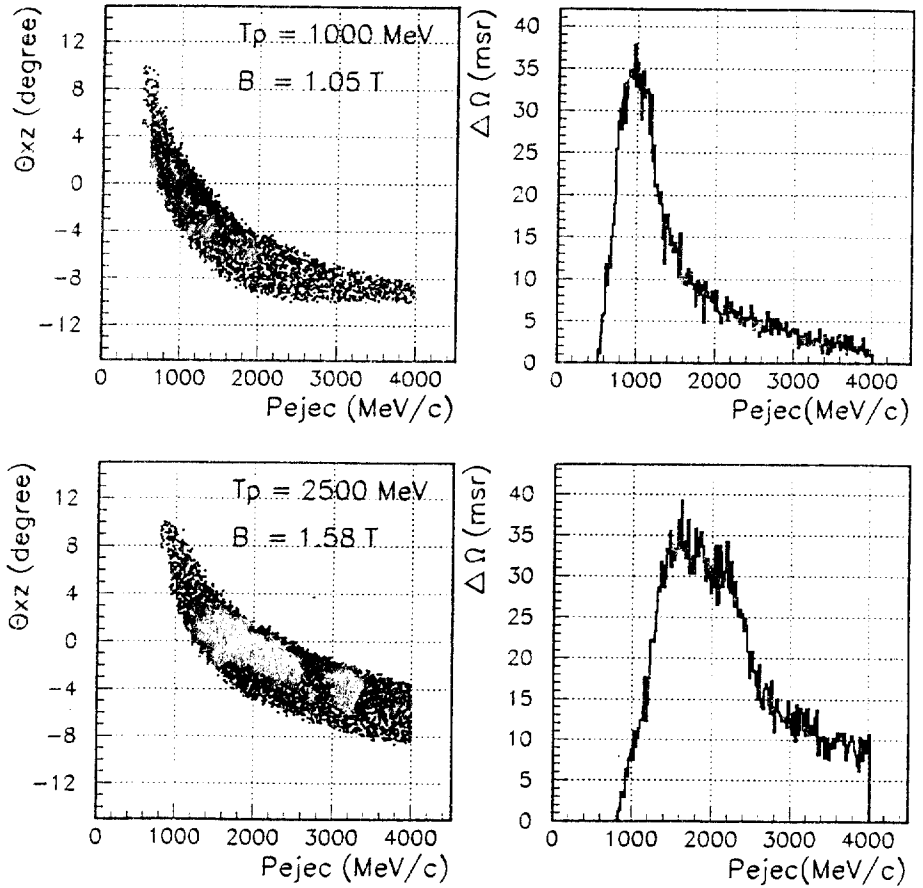


Fig. 1. Layout of the Forward Detector.

## Angular-Momentum Acceptance of the FD



**Fig. 2.** Angular-momentum acceptance of the Forward detector.  $\vartheta_{xz}$ —projection of the polar angle  $\vartheta$  of the ejectile with the momentum  $P_{eject}$  to the median plane XZ of the spectrometer. B is the magnetic field (Tesla) in D2.

**Table 1.** List of the particles detected in FD.

Reaction	$T_p$ [MeV]	Detected particles	$P_{eject}$ [MeV/c]
$p + {}^{12}\text{C} \rightarrow (p, d) + K^+ + X$	800-1400	$p, d$	600-1000
$p + {}^{12}\text{C} \rightarrow (p, d, \dots) + K^+K^- + X$	2000-2500	$p, d, {}^3\text{H}, {}^3\text{He}$	800-3300
$p + d \rightarrow p + p + n$	1000-2500	$p$	800-3300
$p + p \rightarrow d + \alpha_0^+ \rightarrow d + K^+ + \bar{K}^0$	2520-2600	$d$	1000-3400
$p + d \rightarrow d + N^* \rightarrow d + n + \pi^+$	1500-2000	$d$	1000-3000

It is seen that the solid angle acceptance is as large as about 40 msr at the maximum and decreases to 5–10 msr at high momenta. The resulting acceptance is suitable for the experiments of interest (see Table 1).

### Expected Counting Rates .

The background conditions for the processes to be studied were estimated from the Monte Carlo simulation. For event generation the ROC model for pC, pd and pp interactions at different incident proton energy was used. The description of the model can be found in [11]. The code GEANT [12] was used to describe the setup and to trace particles. The other simulation conditions were the same as in [13], [14].

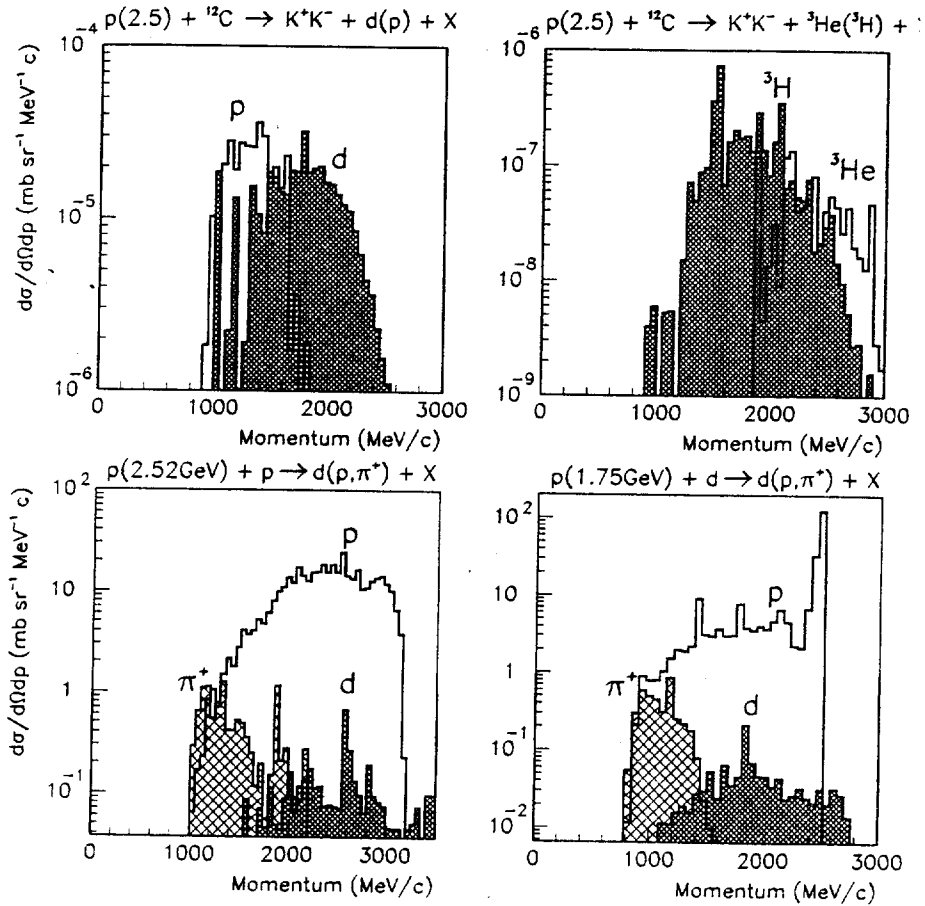
The momentum spectra of secondary particles from the processes (2)–(5), expected in the forward hodoscope, are shown in Fig. 3. It is seen that the particle yield ratios  $N_p : N_d$  and  $N_{3H} : N_{3He}$  are approximately of the same order of magnitude for the process (3) and the yield of three-nucleon fragments is over two orders of magnitude smaller than the yield of p and d. For the reactions  $p + p \rightarrow d(\pi^+, p) + X$  at  $T_p = 2520$  MeV and  $p + d \rightarrow d(\pi^+, p) + X$  at  $T_p = 1750$  MeV the ratio of secondary particles  $N_d : N_\pi : N_p$  is about 1 : 10 : 100.

Table 2 lists inclusive production cross sections for various types of particles produced in the reaction  $p + d \rightarrow d(\pi^+, p) + X$  and detected in the forward hodoscope. The events of pd interactions obtained by the ROC model at the energy  $T_p = 1750$  MeV were used for the estimation. The cross sections expressed in mb are the integrals of the differential cross section over the angular-momentum acceptance with taking into account the detection probability  $\varepsilon_i(\vec{p})$ :

$$\Delta\sigma_i = \int \frac{d^3\sigma}{d\vec{p}} \varepsilon_i(\vec{p}) d\vec{p}.$$

Here the detection probability  $\varepsilon_i(\vec{p})$  is defined only by the angular momentum acceptance of the detector. The cross sections are given separately for deuterons  $\Delta\sigma(d)$  from reaction (5), background protons  $\Delta\sigma_{bg}(p)$  and  $\pi^+$ -mesons  $\Delta\sigma_{bg}(\pi)$  from all other significant  $p + d \rightarrow d(\pi^+, p) + X$  processes detected by the forward hodoscope at  $T_p = 1750$  MeV.

The expected counting rates  $n_i$  can be found multiplying the cross sections  $\Delta\sigma_i$  by the beam-target luminosity  $L$ . At the luminosity  $L = 2.0 \cdot 10^{33} \text{ cm}^{-2} \text{ s}^{-1}$ , expected



**Fig. 3.** Momentum spectra of particles detected in the FD from the processes (2)-(5).

at COSY with the pellet target [6], the total absolute counting rate in the forward hodoscope is equal to  $n = 4.2 \text{ mb} \cdot L \approx 1.0 \cdot 10^7 \text{ s}^{-1}$ .

**Table 2.** Inclusive integrated cross sections (mb) for particles from the reaction  $p + d \rightarrow d(\pi^+, p) + X$  detected in the FD hodoscope counters. The sequential number of the counter increases with increasing the distance from the beam.

$N_{\text{counter}}$	$\Delta\sigma(d)$	$\Delta\sigma_{bg}(\pi^+)$	$\Delta\sigma_{bg}(p)$
#1	0.0006	0.0004	0.804
#2	0.0017	0.0009	0.827
#3	0.0020	0.0022	0.715
#4	0.0022	0.0088	0.675
#5	0.0027	0.0072	0.410
#6	0.0023	0.0064	0.284
#7	0.0011	0.0055	0.214
#8	0.0005	0.0053	0.114
#9	0.0002	0.0052	0.062
Total	0.013	0.042	4.105

### Particle identification .

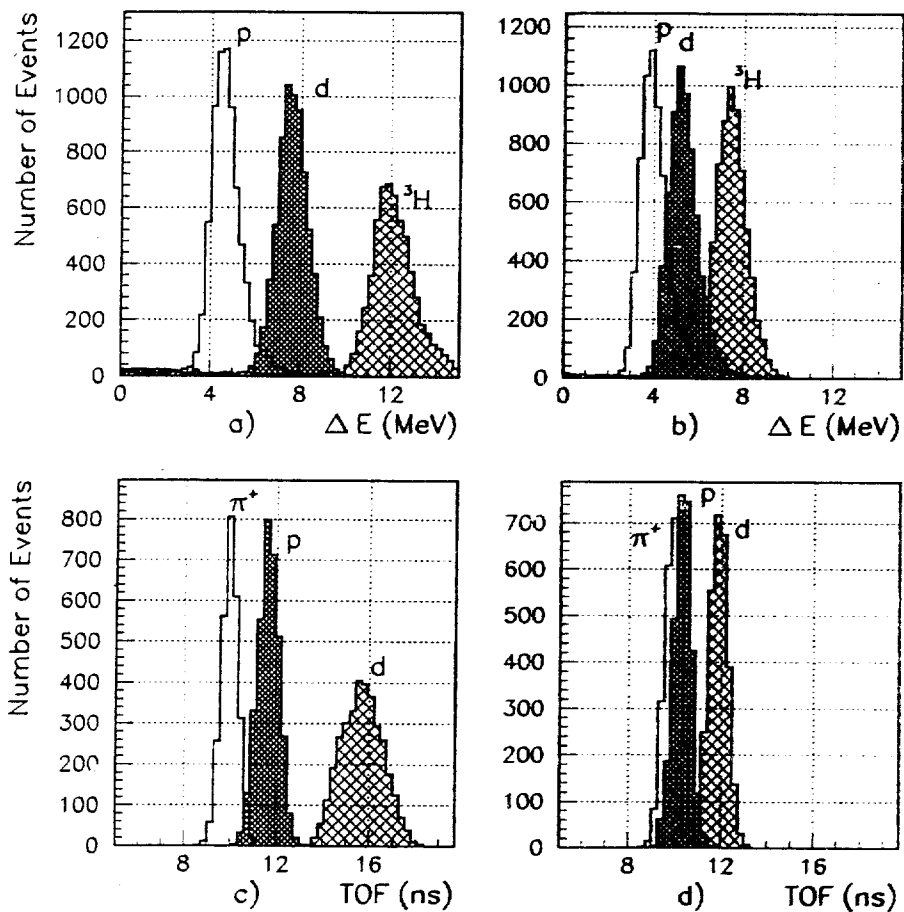
The conditions for deuteron break-up event selection using the particle coincidences in the Forward detector and the Backward detector have been estimated in [13], [14]. In [15], [16] the procedure of  $K^+$  mesons separation from a large pion background in the Side detector has been considered. Let us examine the possibility of separation in the Forward detector the particles ( $p, d, {}^3H, {}^3He$ ), which participate in the processes (2)-(5). The  $\Delta E$  and TOF spectra were simulated to estimate the reliability of identification and the background suppression by the Forward detector elements alone. The uniformly simulated events in the interval of angles  $\vartheta < 10^\circ$  were used as the event generator.

Fig. 4(a, b) displays the distribution of energy losses for the particles ( $p, d, {}^3H$ ) in the forward hodoscope elements (#4 and #8) with the mean momenta of 1500 MeV/c and 2500 MeV/c respectively. The intrinsic energy and time resolution, experimentally measured using the cosmic particles [17], were taken into account. It is obvious that the deposited energy resolution and time resolution of the whole forward hodoscope is better by a factor of  $\sqrt{2}$  when the information from both planes of the hodoscope is used.

Additional background suppression during the off-line data processing using the TOF system has been considered. In Fig. 4(c,d) the time-of-flight distributions for the forward hodoscope elements are presented. The flight time is calculated between the target and a separate forward hodoscope counter. We suppose that the interaction time moment can be reconstructed with the accuracy  $\sigma = 300 \text{ ps}$ . The intrinsic time resolution  $\sigma = 200 \text{ ps}$  for the scintillation counters was assumed [17].



$\pi^+/\rho/d/{}^3\text{H}$  identification in the FD



**Fig. 4.**  $\Delta E$  (a,b) and Time-of-Flight (c,d) spectra for the forward hodoscope counters.

It is seen that this method can be used for  $\pi/p$  separation up to 1500 MeV/c and  $p/d$  separation up to 2500 MeV/c with the background suppression level not worse than an order of magnitude.

Obviously, this is not enough to suppress the proton background at separation of deuterons in processes (4)–(5) because the ratio  $N_d : N_p$  is about 1 : 100 at 2000–3000 MeV/c. Therefore, to improve the  $p/d$  separation we propose to use Cherenkov counters in the Forward detector. A Cherenkov counter based on total internal reflection (CTIR) was proposed and described in [8].

### Background Suppression by Cherenkov Counter .

Fig. 5(a) displays the background suppression factor, namely the proton suppression at detection of deuterons, for a wide momentum range and (b) the corresponding values of the optimum inclination angles. The background suppression factor ( $B$ ) shows the level of background reduction by a Cherenkov counter  $B = \varepsilon_{bg}/\varepsilon$ , where  $\varepsilon_{bg}$  and  $\varepsilon$  are the detection efficiencies for background and useful events respectively at the optimum discrimination threshold.

The background suppression factor was estimated by the Monte Carlo simulation. The Cherenkov light propagation via total internal reflection and the PM output signal generation were simulated by the code GEANT. The Cherenkov light intensity on the PM photocathode is proportional to

$$\sim \eta 2 \arccos\left[\frac{\tan(\vartheta_R + \delta)}{\tan \vartheta_C}\right],$$

where  $\eta$  is the light collection efficiency,  $\vartheta_C$  is the Cherenkov angle,  $\vartheta_R$  is the total internal reflection angle and  $\delta$  is the particle entrance angle. The details of the Cherenkov light yield estimation are described in [8]. The upper curve in Fig. 5(a) corresponds to the light collection efficiency  $\eta = 0.2$  and the lower curve is for  $\eta = 0.6$ , as denoted at the curves.

The PM anode pulses were generated for each event using the Poisson probability density function for photoelectron number distribution and electron multiplication process [18]. The PM characteristics, such as the cathode conversion efficiency, the single electron response relative width and the dark current signal value, were taken for XP2020 [19]. The optimum radiator inclination angle and the discrimination threshold for the PM output signal were obtained for the momentum intervals covered by the individual Cherenkov modules.

It is seen that an addition of the Cherenkov counters to the forward hodoscope leads to reduction of the proton background by more than an order of magnitude.

The proposed Cherenkov module will consist of two identical Cherenkov counters (upper and lower) arranged symmetrically relative to the median plane of the setup. The Cherenkov counters overlap the same solid angle that covered by the forward hodoscope. The total number of Cherenkov counters is 16, the width of each counter is 8 cm, the radiator thickness is 5 cm. All the Cherenkov modules have to be mounted

on the supporting frame allowing to tune the individual module orientation relative to the ejectiles trajectories.

**Total Background Suppression**

It was estimated that with scintillation counters and Cherenkov counters (CTIR), the total background suppression factor is

$$B_{tot} = B_{\Delta E} \times B_{TOF} \times B_{Cher} \approx 10^3 - 10^4$$

and is enough for p/d separation for the momenta up to 3000 MeV/c.

**Conclusion**

The conditions of particle detection in the Forward detector at the spectrometer ANKE have been simulated on the basis of the ROC model data. The simulation results shows that the expected performance of the Forward detector is adequate to requested one in the planned experiments ([2]-[7]).

**Acknowledgment**

Dubna coauthors of the paper are grateful to the Forschungszentrum Jülich and Forschungszentrum Rossendorf and to the members of ANKE Collaboration for the kind hospitality and good working conditions during visits to the centers.

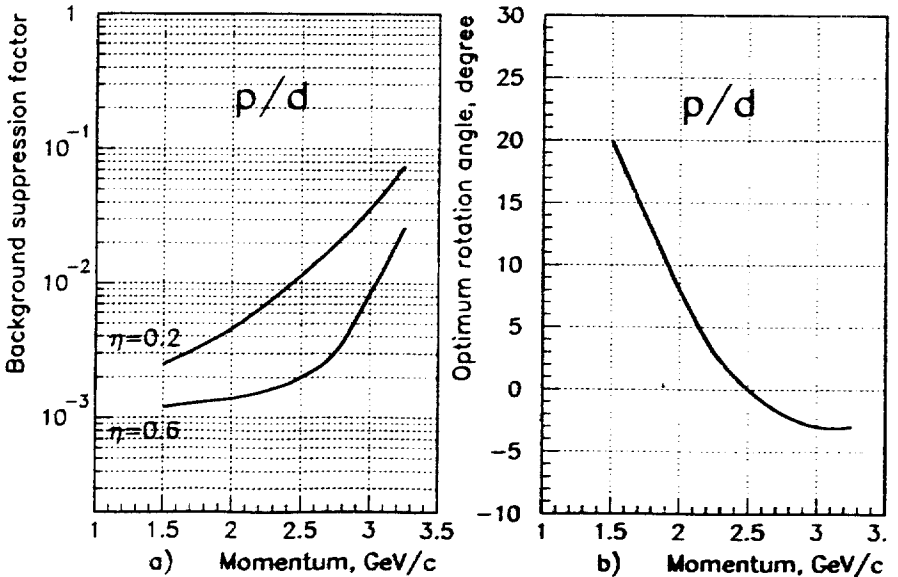


**Fig. 5.** Proton suppression at detection of deuterons:  
 (a) Background suppression factor and (b) the optimum rotation angle.

The present investigation is supported by the RFBR grant No. 96-02-17215.

## References

- [1] V.I.Komarov and O.W.B.Schult, Proc.of the Intern.workshop Dubna, Deuteron-91, JINR E2-92-25, Dubna (1992), p.212
- [2] S.Dshemuhadse et al., COSY Proposal 20, KFA Jülich (1992).
- [3] W.Borgs et al., COSY Proposal 18, Jülich (1992)
- [4] A.A.Sibirtsev, M.Büscher, Z.Phys, A347, (1994), p.191
- [5] H.Müller et al., COSY Proposal 21, KFA Jülich (1996)
- [6] L.A.Kondratyuk et al., COSY Proposal 41, KFA Jülich (1997)
- [7] Yu.N.Uzikov, Yadernaia Fisika vol. 60, N10, (1997), p.1771
- [8] A.K.Kacharava et al., NIM A 376,(1996), p.356
- [9] V.I.Komarov et al., KFA Annual Rep. 1993 Jülich (1994), p.57
- [10] V.I.Komarov et al., KFA Annual Rep. 1995 Jülich (1996), p.67
- [11] H.Müller. Z.Phys, A353, 103, (1995); A353, 237, (1995)
- [12] R.Brun et al.,GEANT Long write-up. CERN, 1993
- [13] A.K.Kacharava et al., JINR report, E1-96-42, Dubna (1996)
- [14] A.K.Kacharava et al., JINR report, E1-96-270, Dubna (1996)
- [15] S.Kopyto, M.Büscher. KFA Annual Rep. 1993 Jülich (1994), p.49
- [16] A.K.Kacharava et al., JINR report, E1-96-505, Dubna (1996)
- [17] V.I.Komarov et al., KFA Annual Rep. 1997 Jülich (to be published)
- [18] B.Bencheikh et al., NIM A 315,(1992), p.349
- [19] Photomultipliers, Data Handbook, PHILIPS, 1990.

Received by Publishing Department  
at 29 October, 1997.

**SUBJECT CATEGORIES  
OF THE JINR PUBLICATIONS**

<b>Index</b>	<b>Subject</b>
1.	High energy experimental physics
2.	High energy theoretical physics
3.	Low energy experimental physics
4.	Low energy theoretical physics
5.	Mathematics
6.	Nuclear spectroscopy and radiochemistry
7.	Heavy ion physics
8.	Cryogenics
9.	Accelerators
10.	Automatization of data processing
11.	Computing mathematics and technique
12.	Chemistry
13.	Experimental techniques and methods
14.	Solid state physics. Liquids
15.	Experimental physics of nuclear reactions at low energies
16.	Health physics. Shieldings
17.	Theory of condensed matter
18.	Applied researches
19.	Biophysics

Качарова А.К. и др.

E1-97-324

Условия регистрации частиц в переднем детекторе  
на установке ANKE

Проведено моделирование условий регистрации частиц в переднем детекторе для установки ANKE (COSY) на основе событий  $pC$ -,  $pd$ - и  $pp$ - взаимодействий, генерированных по ROC-модели в интервале энергий  $T_p = 1000 + 2500$  МэВ. Для подавления протонного фона рассмотрена возможность использования  $\Delta E$ -счетчиков, времяпролетной системы и черенковских счетчиков полного внутреннего отражения.

Работа выполнена в Лаборатории ядерных проблем ОИЯИ.

Сообщение Объединенного института ядерных исследований. Дубна, 1997

Kacharava A.K. et al.

E1-97-324

Expected Conditions of the ANKE Forward Detector Operation

The conditions of the particle detection in the Forward Detector at the spectrometer ANKE (COSY) are simulated on the basis of  $pC$ ,  $pd$  and  $pp$  interaction events generated within the ROC model at the energy range  $T_p = 1000 + 2500$  MeV. The possibility of the background suppression using  $\Delta E$  counters, a TOF system and Cherenkov counters of total internal reflection (CTIR) is examined.

The investigation has been performed at the Laboratory of Nuclear Problems, JINR.

Communication of the Joint Institute for Nuclear Research. Dubna, 1997

Макет Н.А.Киселевой

Подписано в печать 13.11.97  
Формат 60 × 90/16. Офсетная печать. Уч.-изд.листов 1,02  
Тираж 410. Заказ 50271. Цена 1224 р.

Издательский отдел Объединенного института ядерных исследований  
Дубна Московской области